Influence of spindle condition on the dynamic behavior

Mathieu Ritou, Clément Rabréau, Sébastien Le Loch, Benoît Furet, Didier Dumur

https://doi.org/10.1016/j.cirp.2018.03.007

CIRP Template v4.0

Contents lists available at SciVerse ScienceDirect

CIRP Annals Manufacturing Technology

Journal homepage: www.elsevier.com/locate/cirp

Influence of spindle condition on the dynamic behavior

Mathieu Ritou [1], Clément Rabréau [1], Sébastien Le Loch [1], Benoit Furet [1], Didier Dumur (1) [2]

[1] LS2N (Laboratory of Digital Sciences of Nantes, UMR CNRS 6004), University of Nantes, Nantes, France
[2] L2S (Laboratory of Signals and Systems, UMR CNRS 8506), Centrale Supélec, Gif sur Yvette, France

The impact of spindle condition on machining performances is arduous to perceive since very long periods must be considered. This paper proposes an experimental approach based on accurate characterizations of the dynamic behavior for different spindle conditions (repaired or damaged). The Frequency Response Functions of the spindle were obtained for different spindle conditions and speeds, through an electromagnetic excitation device. The main failure modes of HSM spindle were then identified and modeled. Their effects on FRF were simulated and general conclusions were obtained concerning their impacts on spindle dynamics. Lastly, cutting tests reveal the impact of spindle condition on stability lobe diagrams.

Spindle; Wear; Dynamics

1. Introduction

Cutting dynamics is of major importance for the optimization of High Speed Machining (HSM). Moreover, the efficiency of the spindle is also a key point of the machine-tool performance [1]. In particular, spindle dynamics at high speed is of major interest and only partly known. Several electromagnetic devices were developed to investigate experimentally the dynamic behavior [2–4]. Numerical mechanical models were proposed, based on accurate bearing models that consider the dynamic effects [5]. Classical updatings (identification of model parameters) of rotor dynamics model fail, due to too few possible measuring points (compared to classical structural dynamics) and too complex evolutions at high speed. More detailed and phenomenological approaches can provide a better understanding [6-8]. Although the impact of, notably, spindle speed or preload on the Frequency Response Function (FRF) were studied [9-11]; the impact of spindle condition on dynamics has been very rarely examined up to now. HSM spindles are very efficient but also present a high risk of spindle failure [12]. Due to high cost of curative maintenance, spindles are used as long as possible, before their repairs. In this way, partly damaged spindle can produce for months in industry, whereas it has an unknown impact on the cutting dynamics. Besides, it is arduous to perceive since very long periods must be considered. Therefore, there is a strong interest in the investigation of the impact of spindle condition on the dynamic behavior and machining performances.

The paper proposes an original experimental approach based on accurate characterizations of the dynamic behavior for different spindle conditions (repaired or damaged). The FRFs of the spindle were obtained for different spindle conditions and speeds, through an electromagnetic excitation device. The axial behavior was also investigated. The main failure modes of HSM spindle are identified and modeled. Their effects on FRF are simulated and conduct to general conclusions concerning their impacts on spindle dynamics. Lastly, cutting tests reveals the impact of spindle condition on stability lobe diagrams.

2. Experiments

2.1. Procedure

Seven experimental campaigns have been carried out in order to characterize accurately the evolutions of the dynamic behavior of a spindle, in relation to the spindle condition. Four repaired conditions (noted *Rep*) and three damaged conditions (noted *Dam*, just before unmounting for maintenance) of a unique spindle have been studied, over a period of more than three years (Fig.1). There were industrial productions between them. The damaged conditions were determined by the company, notably through vibration measurement.

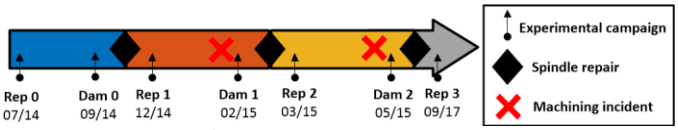

Figure 1. Chronology of the experimental campaigns.

The experiments consist in the measurement of the spindle FRF with an electromagnetic excitation device, at several speeds [2]. A non-contact swept sine excitation of 80 N is applied over a range of 50-5000Hz to a dummy tool. The radial displacement at tool tip is measured by an Eddy current sensor. The radial force is estimated based on a measure of the output current and an identified model of the electromagnetic excitation device [2]. Then, the FRF is computed by H1 formulation.

Besides, the spindle axial behavior is evaluated over a large range of load (-1800 N to +1500 N), during spindle rotations and with an axial loading device [7]. The axial applied force F and the axial shaft deflection (in relation to spindle housing) u are measured and enable the study of the preload and of the axial stiffness evolution with spindle speed. All measures have been performed at the same steady-state operating temperature, at several spindle speeds between 4000 and 24 000 RPM (only results for these extreme values will be presented and discussed).

The studied spindle is a Fischer MFW2310, 70 kW, 24 000 RPM, that consists of 5 hybrid angular contact ball bearings (three SKF VEX70 at the front and two VEX60 at the

rear) in back-to-back arrangements with two spring preload systems (Fig.2). Here, it equips a Huron KX30 machine-tool.

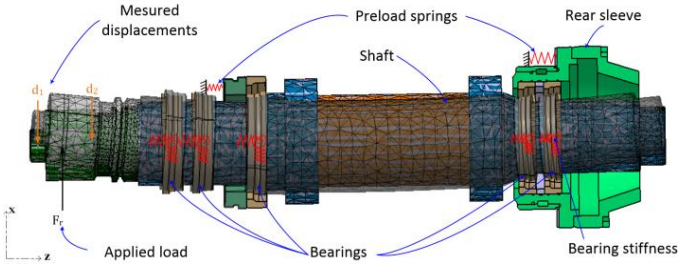

Figure 2. Numerical model of the spindle.

2.2. Results

Figure 3 presents the results of the axial measurements (axial shaft deflection *u* and axial force *F*) at low and high spindle speeds. The different plots refer to the different spindle conditions introduced in Figure 1. At low speed, the slope at low force level shows that there are low variations of the axial stiffness. Note that, contrary to the other ones, Rep0 experiments were conducted over +/-2100 N. More deviations can be observed under -1500 N, where there is a significant drop of the stiffness. It is due to a contact loss in the front bearings. The behavior in this zone is determined by the preload systems and the rear bearings. At high speed, there is no contact loss in the bearings. The axial stiffness (the slope) only differs from one reassembly of the spindle to another one (between colors). The reference of shaft deflection *u*=0µm corresponds to *F*=0N at low speed, for every experimental campaign (see Fig.3). At high speed, the shaft deflects out of the spindle housing (negative vertical displacement *u*), mainly due to centrifugal forces on balls. At *F*=0N, small variations can be observed between repaired spindles. Lower and more dispersed values are obtained for damaged spindles.

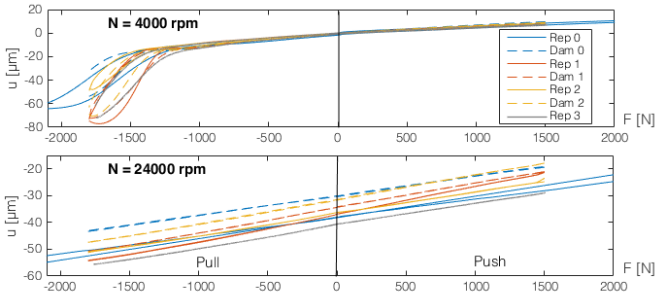

Figure 3. Spindle axial behavior, in relation to the spindle conditions.

The results of radial experiment at low and high speeds with the electromagnetic excitation device are presented in Figure 4. It reveals the dynamic behavior at the tip of the dummy tool.

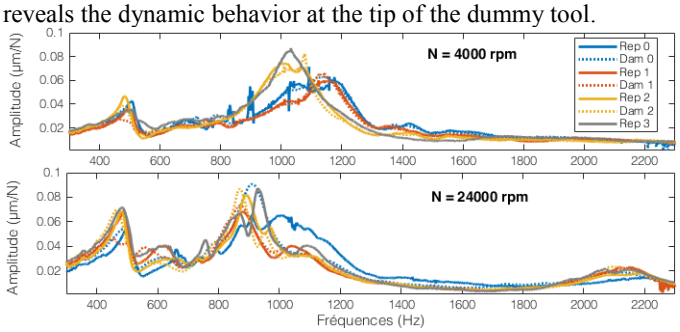

Figure 4. Spindle FRF, in relation to the spindle conditions.

At low speed, eigenfrequencies are visible at around 500 and 1100Hz. The frequency of the mode at 500Hz is constant with speed, but the other frequencies are evolving due do dynamic effects. Some modes appear at high speed (at 600 and 2100Hz).

It has been verified that the observed effects are greater than the variability of the experiment. According to the spindle condition, it can be noted that relatively similar FRFs are obtained. It is quite logical since the major design characteristics of the spindle, such as the shaft dimensions and the bearing types and positions, remain identical over time. However, interesting and non-negligible variations of the dynamic behavior can be observed.

Larger deviations are obtained between reassemblies of the spindle, rather than between repaired and damaged conditions. Notably for Rep2 and Rep3, at low speed, the dominant mode (which is at 1150Hz for Rep0 and Rep1) has switched with the 1000Hz mode due to evolutions of mode coupling. This phenomenon is also visible at high speed, for Rep0. The frequency of the 500Hz mode is almost constant, but its amplitude decreases for Dam1 damaged spindles. The frequency can also vary, as for Dam2 at 900Hz at high speed.

Therefore, spindle dynamics can be affected by the spindle condition and, paradoxically, by the reassemblies.

2.3. Failure modes of HSM spindle

In order to explain the observed evolutions of FRF, the main failure of HSM spindle need to be identified and modeled. In a FMEA conducted in UsinAE project, around 250 reports of repairer's diagnostic at disassemblies of this spindle (used in aeronautic industry) had been analyzed. It revealed that the main failure modes of HSM spindles are, in order of importance: faulty ball bearings, modified geometry of HSK or shaft, defective bearing lubrication, clamping system or cooling system [13]. Note that, during any spindle repair, all bearings are changed (because they are damaged before or during disassembly) and preload is adjusted, to meet the manufacturer's specifications.

Concerning the failures of Dam0, Dam1 and Dam2, several ball bearings were systematically damaged (at front or rear bearings) and presented a white strip on the contact zone of raceways, which is common for aluminum HSM spindles in aeronautics [12]. Bearing lubrication was defective for Dam0. Components of the tool clamping system and of the rotary union were worn for Dam0 and Dam1. Dimensions were out of tolerance (of several microns) concerning the HSK interface (Dam0&1) and the shaft (Dam0). Thus, the observed damaged spindles are representative of the main failures of HSM spindle.

We have investigated the failure of a Dam1 rear bearing, due to a tool breakage (Fig. 5). The raceways were measured with Alicona Infinite Focus. The worn white strip is a distributed defect on the whole circumference of the contact zone on the raceways with an areal roughness Sa=936µm (versus 643nm for unworn zone). It consists of a number of micro-indentations, of an average depth of -5µm. This bearing failure mode is a false-brinelling and it is due to the intensive vibrations [14].

The main failure modes of HSM spindle are henceforth known and models can be proposed to predict their effects on dynamics.

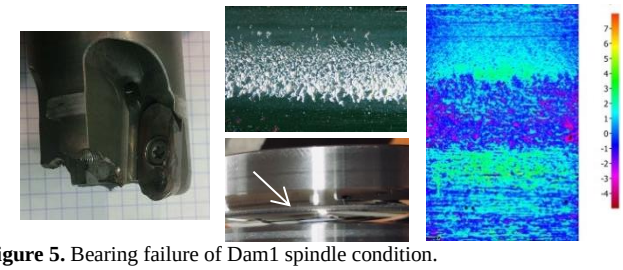

Figure 5. Bearing failure of Dam1 spindle condition.

3. Modeling of the spindle condition

3.1. Spindle model

The main components of the numerical simulations are presented in Figure 2. The shaft and the dummy-tool are modeled by 3D finite-elements. Mass and stiffness have been added on the location of the motor with 2D finite elements. The spindle housing is considered flexible and modeled by 3D finite-elements. The ball bushing between the rear sleeve and the spindle housing is modeled by a 5DoF spring joint: the preload springs in the axial direction and a 2x2DoF for rotations and translations in each radial direction. The machine-tool dynamics is modeled by a 2x2DoF joint, of which modal parameters are identified for the two principal modes of the machine-tool in each radial direction. The HSK interface is modelled by 2x2DoF stiffness. LMS Virtual.Lab software using linearized temporal computations were used for the multi-body dynamics simulations.

The bearings behavior is taken into account through 5x5 stiffness matrix that depends on the spindle speed. These matrices are obtained by the updating of the analytical model of the spindle axial behavior. It is based on a 5DoF model of the angular contact ball bearings [15]. Based on axial experiments (Fig.3), a model update of the axial equilibrium of the preloaded system is performed. It provides the operating preload (force and stiffness) values and other bearing parameters with regards to the speed and the axial load [7]. The preload systems and arrangement of bearings (with identified values) are integrated in the 3D model. The phenomenological model takes into account the dynamic effects in the bearings: centrifugal forces and gyroscopic moments on balls, and also macroscopic deformations of the shaft due to dynamic and thermal effects. The presence of a stroke limit and of friction between the rear sleeve and the housing is considered.

The transparent grey shaft in Figure 2 illustrates the spindle dominant mode, which is a shaft bending mode. Simulations of the 3D spindle model are in good agreement with the electromagnetic device FRF, particularly at high speeds.

3.2. Phenomenological modeling of spindle wear

The aim is to propose a model of the main failure modes of HSM spindle. It is used to investigate the impact of these failures on the dynamic behavior of HSM spindle. In order to understand the complete variability of spindle dynamics, not only failures are considered (evolution from repaired to damaged condition), but also the spindle repairs (variability between reassemblies). Variation ranges of parameters were chosen below based on experimental observations and literature.

Modified preload. The axial experiments have shown variation of the preload, particularly between reassemblies (Fig.3). Indeed, bearings are changed at each spindle repair. They are mounted with interference fit on the shaft and the preload is adjusted again, to meet the specification for the considered spindle. However, unwitting variation of preload force can be observed, due to tolerance stack that slightly modifies the springs compression. Preload springs are also sometimes changed (e.g. for Rep1). Consequently, this variability is modeled through modified values of preload force and preload spring stiffness. It modifies the axial equilibrium of the bearings arrangement and the new bearing stiffness matrixes are computed for the spindle 3D model. The impact of a preload variation has been studied. Figure 6 present the results for preloads of $1700N^{+/-200N}$. It is shown that variations of the preload force have a noticeable effect on all the spindle modes, modifying eigenfrequency and amplitude. Besides, lower spring stiffness decreases the main eigenfrequency and also modifies amplitudes.

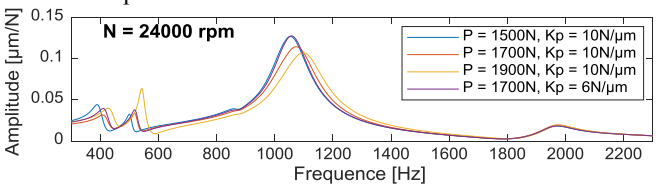

Figure 6. FRF simulations with modified preload.

Deformed raceway of bearing. Due to wear or false-brinelling, the geometry of the bearing raceway can have been modified. Indeed, false-brinelling causes distributed defects on the entire raceway circumference, by vibrations-induced indentation. It modifies the ball-raceway contact. It can be modeled with a different value of raceway groove curvature radius in the bearing model. Two hypotheses have been formulated: the groove radius can have been increased around the contact zone by plastic deformations at a macroscopic scale; or micro-indentation has conducted to a smaller local groove radius, close to ball radius. Both hypotheses modify the bearing stiffness matrixes. Figure 7 presents the simulation results for +3% variation of the outer raceway groove radius, for front or rear bearings. It mainly modifies the amplitudes of the modes. Defective front bearings mainly affect the main mode, at 1000Hz; whereas defective rear bearings affect lower frequency mode, at 600Hz.

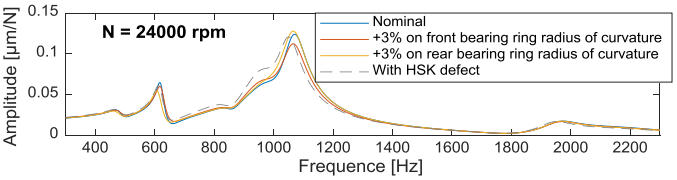

Figure 7. FRF simulations for faulty bearings or HSK interface.

Modified bearing lubrication. The distributed micro-indentation induced by false-brinelling degrades the roughness at the ball-raceway contact, as observed in Figure 5. It has an impact on the bearing lubrication, particularly the oil film thickness, which modifies the bearing damping [16,17]. The consequence of an increased damping (from 12% to 22%) in the front or rear bearings has been studied. Figure 8 shows that defective front and rear bearings significantly modify the amplitude of the dominant mode, which is a shaft bending mode the but front and rear bearings also contribute. A defective rear bearing significantly decreases the amplitude of the 600Hz mode (rear sleeve mode).

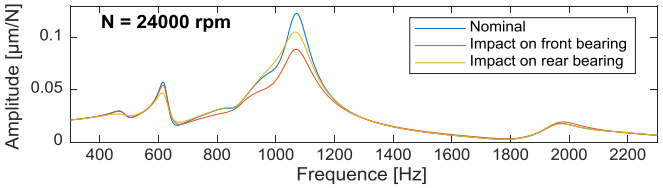

Figure 8. FRF simulations with increased bearing damping.

Defective tool clamping. Components of the tool clamping system can be worn or a lack of grease can modify the friction. As a consequence, the clamping force can be reduced, which decreases the stiffness at the HSK interface. Wang et al. [18] have observed experimentally a stiffness drop of 67% for a clamping of 5kN (instead of 18kN). However, these variations are visible only if the angular deflections are large enough. Introducing Wang's values in the spindle model, Figure 7 shows that a 67% drop of the 2x2DoF HSK stiffness has a limited impact on the principal modes, whereas an extremely low clamping force was used.

Unbalanced rotor

After shocks, the balance of the rotor components assembly can be modified. It can be modeled by an additional mass on the shaft. The spindle temporal simulations have shown that small unbalance have no effect on the FRF. Only an increased contribution at the spindle frequency can be measured in the vibration spectrum.

4. Discussion

The experimental results can henceforth be analyzed and understood through the dynamics simulations with models of the main failure modes of HSM spindle. Paradoxically, the most significant changes of spindle dynamics that have been observed are not due to a worsened spindle condition, as expected, but they are due to preload variations at spindle reassembly. Indeed, a +100N increase (from 1700 to 1800N) of the preload force has been identified with the axial experiments for Rep2. It modifies the bearing stiffness matrices and the couplings around the dominant bending mode at 1000Hz. However, the spindle condition has also a noticeable impact on the spindle dynamics. The variations are mainly explained by bearing failures and the deterioration of their raceways. Compared to Rep1, Dam1 spindle dynamics presented lower amplitude for the rear sleeve mode at 500Hz (Fig.4). Thus, the distributed false-brinelling that is common and was observed on bearing seems to increase the damping, as simulated in Figure 8.

As a synthesis, the major effect is due to the preload variation between spindle reassemblies that modifies the frequency and amplitude of the dominant mode, through bearing stiffness. Faulty bearings mainly affect the modes amplitude, through increased damping. The rear bearing has a great impact on the rear sleeve mode (at 600Hz); both front and rear bearings have a lower effect on the dominant bending mode amplitudes (at 1000Hz); and front bearing on the higher frequency bending modes. The frequency shift between repaired and damage conditions is mainly explained by the degraded HSK that modifies the tool-shaft bending.

5. Impact on cutting dynamics

Experiments were performed in order to investigate the impact of the spindle condition (Dam1 VS Rep2) on cutting dynamics. A shrink-fitted 20mm diameter, 176mm long and 2 teeth carbide tool was chosen for milling 7050 aluminum alloy.

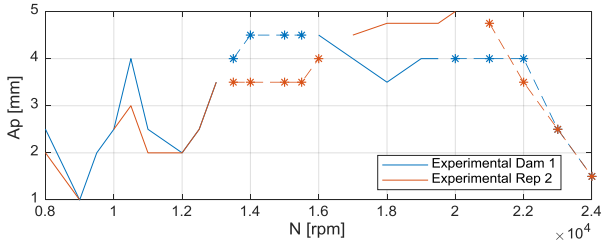

Figure 9. Impact of spindle condition on stability lobes diagrams.

Figure 9 presents the stability lobes diagrams (SLD) that were obtained. Note that around 15 and 22kRPM, instability could not be reached due to excessively high vibration levels (asterisks). Elsewhere, a significant effect of spindle condition on cutting dynamics is revealed. At 10 000 RPM, the stability limit increases of 33% for Dam1 damaged spindle condition. Conversely, the stability limit drops of 26% at 18 000 RPM. Consequently, spindle condition can significantly degrade the quality of industrial production.

6. Conclusion

An original approach has been proposed for the study of the impact of spindle condition on the spindle dynamics. 7 experimental campaigns were performed over 3 years, with accurate characterization of the dynamic behavior with an electromagnetic device. The main failures modes of HSM spindle were identified (bearing false-brinelling notably) and modeled. Their effects on FRF were simulated and general conclusions were obtained concerning their impacts on spindle dynamics. Paradoxically, the major effect is due to preload variation between spindle reassemblies (for which additional attention should be paid). Faulty bearings mainly modify mode amplitudes and a degraded HSK modifies the frequencies of bending modes. The significant impact of spindle condition on cutting stability was also observed.

Acknowledgment

This research was supported by the French FUI QuaUsi project. The authors thank Europe Technologies and Precise companies for their contribution.

References

[1] E. Abele, Y. Altintas, C. Brecher, Machine tool spindle units, CIRP Annals - Manuf. Technol. 59 (2010) 781–802. doi:10.1016/j.cirp.2010.05.002.

[2] D. Tlalolini, M. Ritou, C. Rabréau, S. Le Loch, B. Furet, Modeling and characterization of an electromagnetic system for the estimation of Frequency Response Function of spindle, Mech. Syst. Signal Process. 104 (2018) 294–304. doi:10.1016/j.ymssp.2017.11.003.

[3] A. Matsubara, T. Yamazaki, S. Ikenaga, Non-contact measurement of spindle stiffness by using magnetic loading device, Int. J. Mach. Tools Manuf. 71 (2013) 20–25. doi:10.1016/j.ijmachtools.2013.04.003.

[4] M. Rantatalo, J Aidanpaa, B Goransson, P Norman, Milling machine spindle analysis using FEM and non-contact spindle excitation and response measurement, Int. J. Mach. Tools Manuf. 47 (2007) doi:10.1016/j.ijmachtools.2006.10.004.

[5] H. Cao, L. Niu, S. Xi, X. Chen, Mechanical model development of rolling bearing-rotor systems: A review, Mech. Syst. Sign. Proc. 102 (2018) 37–58.

[6] Y. Cao, Y. Altintas, A General Method for the Modeling of Spindle-Bearing Systems, J. Mech. Des. 126 (2004) 1089. doi:10.1115/1.1802311.

[7] C. Rabréau, D. Noël, S. Loch, M. Ritou, B. Furet, Phenomenological model of preloaded spindle behavior at high speed, Int. J. Adv. Manuf. Tech. 90 (2017). doi:10.1007/s00170-016-9702-1.

[8] J. Jedrzejewski, W. Kwasny, Modelling of angular contact ball bearings and axial displacements for high-speed spindles, CIRP Annals 59 (2010) 377-382.

[9] H. Cao, T. Holkup, Y. Altintas, A comparative study on the dynamics of high speed spindles with respect to different preload mechanisms, Int. J. Adv. Manuf. Technol. 57 (2011) 871–883. doi:10.1007/s00170-011-3356-9.

[10] A. Zivkovic, M. Zeljkovic, S. Tabakovic, Z. Milojevic, Mathematical modeling and experimental testing of high-speed spindle behavior, Int. J. Adv. Manuf. Technol. (2014). doi:10.1007/s00170-014-6519-7.

[11] E. Ozturk, U. Kumar, S. Turner, T. Schmitz, Investigation of spindle bearing preload on dynamics and stability limit in milling, CIRP Annals 61 (2012) 343–346. doi:10.1016/j.cirp.2012.03.134.

[12] C. De Castelbajac, M. Ritou, S. Laporte, B. Furet, Monitoring of distributed defects on HSM spindle bearings, Appl. Acoust. 77 (2014) 159–168. doi:10.1016/j.apacoust.2013.07.008.

[13] E. Maleki, F. Belkadi, M. Ritou, A. Bernard, Tailored ontology supporting sensor implementation for the maintenance of industrial machines, Sensors 17 (2017) doi:10.3390/s17092063

[14] SKF, Railway technical handbook, Vol. 1, Bearing Investigation, (2012) http://www.skf.com/binary/86-62751/RTB-1-06-Bearing-investigation.pdf.

[15] D. Noel, M. Ritou, B. Furet, S. Le Loch, Complete Analytical Expression of the Stiffness Matrix of Angular Contact Ball Bearings, J. Tribol. 135 (2013) 41101. doi:10.1115/1.4024109.

[16] M. Sarangi, B.C. Majumdar, a S. Sekhar, Stiffness and damping characteristics of lubricated ball bearings considering the surface roughness effect. Part 2: numerical results and application, Proc. Inst. Mech. Eng. Part J J. Eng. Tribol. 218 (2004) 529–538. doi:10.1243/1350650042794716.

[17] P. Dietl, J. Wensing, G.C. van Nijen, Rolling Bearing Damping for Dynamic Analysis of Multi-body Systems-experimental and Theoretical Results., J. Multi-Body Dyn. (2000) 33. doi:10.1243/1464419001544124.

[18] G.C. Wang, S.L. Wang, W.G. Wu, C.G. Shen, Stiffness of HSK Tooling System in High Speed Machining, Mater. Sci. Forum. 505–507 (2006) 469–474. doi:10.4028/www.scientific.net/MSF.505-507.469.